Journal of Bone and Mineral Metabolism (2019) 37:1048–1057
https://doi.org/10.1007/s00774-019-01011-1

ORIGINAL ARTICLE

Functional disuse initiates medullary endosteal micro-architectural impairment in cortical bone characterized by nanoindentation

Kartikey Grover[1] · Minyi Hu[1] · Liangjun Lin[1] · Jesse Muir[1] · Yi-Xian Qin[1]

Received: 28 April 2017 / Accepted: 16 May 2019 / Published online: 10 July 2019

Abstract

In this study, we evaluated the effect of functional disuse-induced bone remodeling on its mechanical properties, individually at periosteum and medullary endosteum regions of the cortical bone. Left middle tibiae were obtained from 5-month-old female Sprague–Dawley rats for the baseline control as well as hindlimb suspended (disuse) groups. Micro-nano-mechanical elastic moduli (at lateral region) was evaluated along axial (Z), circumferential (C) and radial (R) orientations using nanoindentation. Results indicated an anisotropic microstructure with axial orientation having the highest and radial orientation with the lowest moduli at periosteum and medullary endosteum for both baseline control as well as disuse groups. Between the groups: at periosteum, an insignificant difference was evaluated for each of the orientations ($p > 0.05$) and at endosteum, a significant decrease of elastic moduli in the radial ($p < 0.0001$), circumferential ($p < 0.001$) and statistically insignificant difference in axial ($p > 0.05$) orientation. For the moduli ratios between groups: at periosteum, only significant difference in the Z/R ($p < 0.05$) anisotropy ratio, whereas at endosteum, a statistically significant difference in Z/C ($p < 0.001$), and Z/R ($p < 0.001$), as well as C/R ($p < 0.05$) anisotropy ratios, was evaluated. The results suggested initial bone remodeling impaired bone micro-architecture predominantly at the medullary endosteum with possible alterations in the geometric orientations of collagen and mineral phases inside the bone. The findings could be significant for studying the mechanotransduction pathways involved in maintaining the bone micro-architecture and possibly have high clinical significance for drug use against impairment from functional disuse.

Keywords Nanoindentation · Orientation · Periosteum · Endosteum · Micro-architecture

Introduction

Shear forces imparted by the movement of bone fluid on osteocytes inside the canaliculi is one of the possible mechanotransduction pathways, which further leads to increased bone formation [1–9]. Research indicates that cyclical loading causes a gain in the mechanical strength of bone, and the absence of loading causes loss of bone mechanical strength [1, 3, 10–16]. Previous studies also show that functional disuse impairs bone micro geometrical properties and mineralization [17–19]. Patients of functional disuse could be astronauts on long-term space flights or patients of whole body paralysis or long-term bed rest [20]. At the micro level, the mechanical competence of bone is due to a combination of collagen fibrils and crystalline mineral hydroxyapatite [21]. Research has shown that an increase in mineralization density leads to an increase in bone elastic moduli [22]. It is also demonstrated that regional collagen fiber orientation is positively correlated to the regional tensile strength of cortical bone [23–25]. Martin and Boardman showed that 62% of bone moduli variability was due to collagen fiber density, orientation, and porosity [23]. More recently, Bouxsein in her studies, analyzing various contributory factors of fracture risk in the human hip bone, showed that not just areal bone mineral density (aBMD), but also the micro-architecture of the bones has a significant effect on fracture risk and its propagation [26]. It was proposed that the spatial distribution of bone mass, intrinsic properties of bone material and micro-architecture all together determine bone strength and its resistance to fracture [27]. Research by Fan's group on sheep tibia bone recovering from a fracture, displayed

✉ Yi-Xian Qin
yi-xian.qin@stonybrook.edu

[1] Department of Biomedical Engineering, SUNY Stony Brook University, 215 Bioengineering Building, Stony Brook, New York 11794, USA

that bone microstructure and spatial distribution altered during remodeling from the healing process [28]. Other studies also show that trabecular bone exhibits an altered micro-architecture and variation in the degree of anisotropy from changes in mechanical loading and generated adaptation [29]. These studies advance that it might not be just the bone mineral and collagen density, but also its micro-architecture, which determine the bone's load bearing ability. Being important indicators of bone health, how they are affected in the microscale by functional disuse, is one of the prime motives of this study.

From the micro to the macro scale, bone has a complex hierarchical structure [30, 31]. In a single bone transverse cross-section, the range of micro-mechanical properties can be observed [32–34]. The outer periosteal side of bone is the bone-forming layer. The periosteum consists of two separate layers; the outer fibrous layer and the inner cellular layers [35, 36]. While the outer layer is highly vascularized, the inner layer has a high osteogenic potential [37]. The inner layer is formed by a thin membrane of connective tissue connected to the medullary cavity and termed as the endosteum. Investigations by Seeman and his group showed that osteoporotic conditions cause an increase in remodeling rate, which causes an increase in the endosteal resorption and thereby causing a further decrease in cortical thickness and loss of structural index [38, 39]. Mechanical loading has shown to increase bone surface remodeling at both periosteal and endosteal surface, as well as an increase in bone mineralization [40]. In another study, it was displayed that exercise and mechanical loading increased periosteal perimeter and periosteal mineral apposition rate in mice tibiae [41]. Considering the high remodeling sensitivity of the periosteum and endosteum, they were identified as the investigation regions for this study. For consistency, all indentations were carried out in the lateral side of all the bones.

In addition to a range of micro-mechanical properties in a cross-section, bones also have a high degree of anisotropy. Usually, the weight-bearing bones have a higher modulus in the longitudinal orientation so that they can sustain the high compressive loads being applied during walking, running, and other activities [42]. In addition to the macro anisotropy a distinct micro level anisotropy has also been observed. Nanoindentation makes the investigation of mechanical properties such as elastic moduli and hardness possible at micro and nano levels [34, 43–48]. Research by Fan and Khadaker [45, 49] showed that bone has a definite anisotropy in its mechanical properties at the micro level. Previous research by Reisinger et al., Franzoso et al., Faingold and Carneli measured the anisotropy of single primary and secondary osteons in cortical bone using nanoindentation techniques [50–53]. Reisinger signified that in cortical bone, osteons have higher axial moduli, against the twisted plywood structure of collagen fibers. Fransozo's group also measured single secondary osteon anisotropy and revealed they were too stiffer in the axial orientation.

In spite of the extensive past research, very few studies so far, have focused on the elastic moduli in the three orientations-axial, circumferential and radial and the anisotropy ratios separately at periosteum and endosteum.

The central hypothesis behind the study was that disuse-induced osteopenia would cause region specific bone remodeling with an initiating at the endosteum. Hence, the first objective of the study was to evaluate and compare the elastic moduli at both periosteum and medullary endosteum for both our control and disuse groups. Our secondary hypothesis was that functional disuse-induced osteopenia would cause an initial remodeling in the bone micro-architecture. Thus, the second objective was to analyze the effects of functional disuse on the micro-mechanical moduli ratios, i.e., the Z/C, Z/R, and C/R ratios for both the control and disuse bones. A significant difference between the moduli ratios between control and disuse bone would complement the result.

The model used in this study for the investigation of bone remodeling from functional disuse was a rat hind limb suspension model. As during hind limb suspension, the hind limb bones experience gravity-free situations, they would suffer from disuse-induced osteopenia [54, 55].

Materials and methods

Left tibia bone samples were obtained from 5-month old virgin female Sprague–Dawley rats, including 1) baseline control ($n=9$), and 2) hind limb suspended (HLS) (4 weeks, $n=9$)from a previous study of the group [54]. During the hind limb suspension procedure in the previous study, rats were suspended using a tail harness and a swivel hook using surgical tapes. The rats had approximately 30° of head-down tilt and their hind limbs were approximately 2 cm from the ground. The body weight of the animals was monitored 5 times per week throughout the study. Stony Brook University IUCAC had previously approved the animal study.

Sample preparation

For the axial orientation, 2 mm thick segments were cut from the middle of the tibia bone in the transverse plane, using a diamond coated rotating cutter saw blade (South Bay technology Inc., MODEL 650, Clemente, California, USA) under constant water irrigation (Fig. 1). For the circumferential orientation, 4 mm thick segments were cut again from the middle of the tibia but in the coronal plane (Fig. 1). An indent mark was made on the lateral side. And finally, for the radial orientation- 3 mm thick segments were again cut from the middle of the tibia bone in the

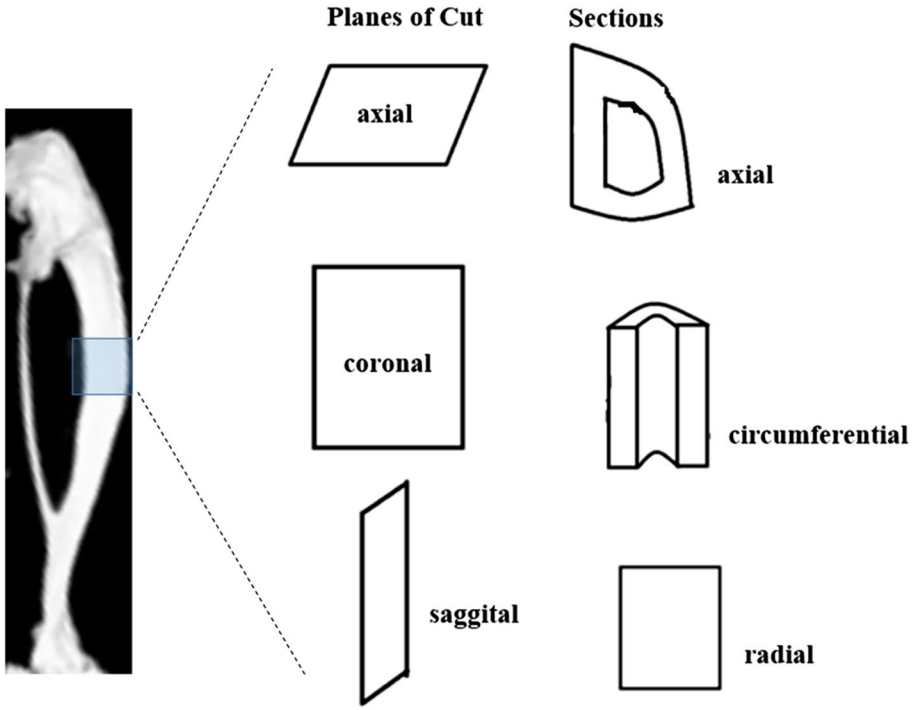

Fig. 1 Showing the schematic of cutting of a tibia bone in three mutually orthogonal planes, i.e., the axial, coronal and sagittal planes so that the axial, circumferential and radial orientations are obtained for indenting. A diamond saw cutter blade was used for cutting of the tibia bone

sagittal plane (Fig. 1). An indent mark was made on the periosteal region of the bone. Twice the numbers of cuts were made for the radial orientation to have the same number of radial orientation samples as other orientations both on the periosteal and endosteal side. The bone marrow was cleared using a water jet. As the bone segments were in the order of millimeters, differences of moduli along the length of the tibia were assumed to be minimal.

Embedding and polishing of samples

For complete dehydration, bone samples were stored in ethanol of subsequent higher concentrations of 70%, 80%, 90% and then 100% each for 2 days. Afterward, the bone samples were embedded in epoxy resin and let to cure for a day. Subsequently, the embedded samples were first polished with silicon carbide papers (Buehler-Carbimet, Illinois, USA) of grit no. 320, 600, 1200, 2400 and finally by 4000 on a Buehler grinder Power pro 3000™ (Illinois, USA) in the respective ascending order. For the radial direction, directly grit no. 1200 silicon carbide was used for grinding and then subsequent higher order carbide papers were used, i.e., 2400 and 4000. Great care was taken to expose just the surface, and extremely shallow grinding was employed. Finally, the samples were polished by Polycrystalline Diamond Suspensions (Buehler MetaDi™ Supreme) of roughness 3 µm, 1 µm, 0.25 µm and finally by 0.05 µm in the given descending order.

Nanoindentation

The distribution of elastic modulus was measured on a micro scale by Nanoindentation (Hysitron Triboindenter TI-950, Minneapolis, Minnesota) at precise locations. Tip of the nanoindenter was a Berkovich tip. All indentations were carried out on the lateral region of bone for consistency.

For the axial and circumferential orientations, indents were made near the periosteum, middle and also near the endosteum of the bone in the lateral side, as shown in Fig. 2a, b. In the radial orientation for both the periosteal and endosteal regions, indents were made at 4 sites which were more than at least 100 µm away as shown in Fig. 2c. The points of indentation on the bone were chosen after viewing the cross-section under the imaging system of the Triboindenter (Hysitron, Inc.), which comprised of an objective of magnification 10× and an eyepiece of magnification 2×. No further magnification was needed to select points for indentation. The tip area function was calibrated from indentation analysis on fused quartz, and drift rates in the system were measured prior to each indentation using standard indentation testing procedures. A preload of 2 µN was used before indentation. The indentation consisted of 10 s of loading period at a constant loading rate of 100 µN/s. A constant load segment at the peak load of 1000 µN followed this for a time of 30 s. Afterward, the tip was retracted in the unloading segment for another 10 s at a constant unloading rate of 100 µN/s. The total indentation time was 50 s. The indentation procedure consisted of a 3 × 3 pattern, for each

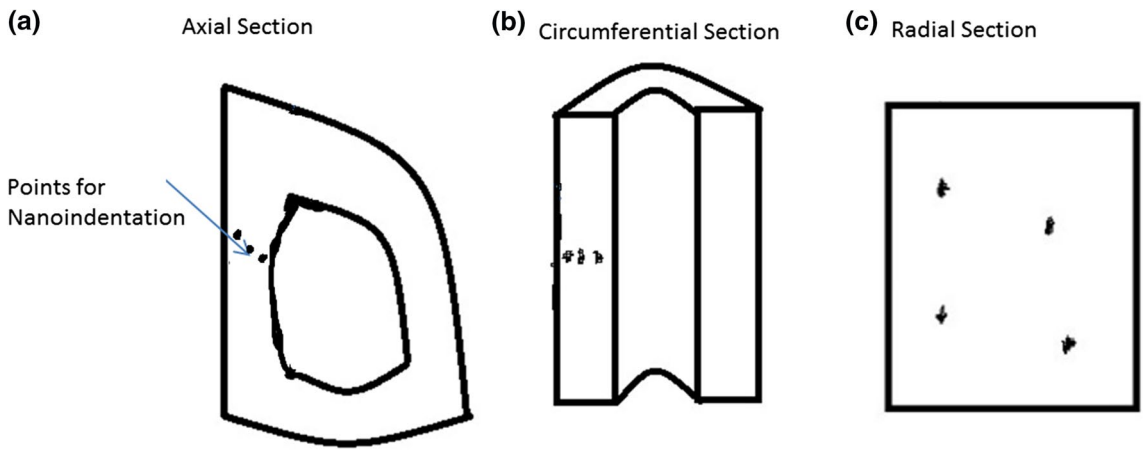

Fig. 2 Schematic showing the three orientations-axial, circumferential, and radial for indenting. The black dots resemble the indentation points. All indents are performed on the lateral region of the bone. In the radial orientation indentation points were at least 100 µm away from each other

indent point. The elastic response was calculated from the 20–90% portion of the unloading curve. Elastic modulus was calculated assuming an elastic response during unloading and using Oliver Pharr Method [56]. The values of elastic modulus were noted for each indent.

Statistical analysis

The data from the Tribo Scan software of Hysitron Triboindenter were exported into Microsoft Excel (Microsoft Excel 2011, version 14.0.0). Two-tailed unpaired Student's *t*-test was performed when the control and disuse groups were compared for each of the circumferential, radial and axial orientations. One-way ANOVA test, IBM statistical software SPSS 22.0, was performed for comparing the elastic moduli of all the three-axial, circumferential and radial orientations in both the control and disuse groups. Further Tukey test post hoc pairwise testing was performed to find statistically significant differences amongst the orientations (axial, circumferential and radial) after One-way ANOVA in SPSS. To compare the Z/C, Z/R or C/R ratios between the control and the disuse groups at both the periosteum and medullary endosteum, unpaired Student's *t* test was performed. The significance level was set at 0.05 for the *t*-tests, One-way ANOVA tests, and Tukey post hoc analysis tests. All the bar charts were plotted in Excel.

Results

Animal weight

The animal weight results are reported from the previous study of the group. The average weight of the animals of the control and functional disuse groups was not statistically different at the beginning of the study and was roughly 305 ± 16 g. The control group rats maintained a steady weight throughout the study and had an average difference of $+4.7\%$ between the start and end dates. But the disuse group after 4 weeks of hind limb suspension lost a significant amount of weight (-5%; $p < 0.05$).

Variation of moduli at periosteum and endosteum in different orthogonal orientations

In both the control and disuse groups, it was observed that the Z or axial orientation had the highest modulus, followed by circumferential and then least in the radial as shown in Fig. 3. The mean modulus values in the axial, circumferential and radial orientation were 27.20 GPa, 22.58 GPa, and 20.24 GPa, respectively for the control group and 27.85 GPa, 22.16 GPa, and 18.79 GPa, respectively for the disuse group. The mean moduli were calculated as the average of the periosteal, middle and endosteal indent for a particular orientation. Figure 3a shows the periosteal moduli in both control and disuse groups and Fig. 3b shows the endosteal moduli for both the control and disuse groups. The pattern was similar for both the periosteal and endosteal sides of the bone. There was a statistically significant difference among the elastic moduli of the three orientations ($p < 0.05$) from the results of the one-way ANOVA test. Pairwise post hoc analysis further showed that each orientation was statistically significantly ($p < 0.05$) different. Similar trends were observed at both the periosteal and the endosteal regions of the bone and also for both the control and disuse groups.

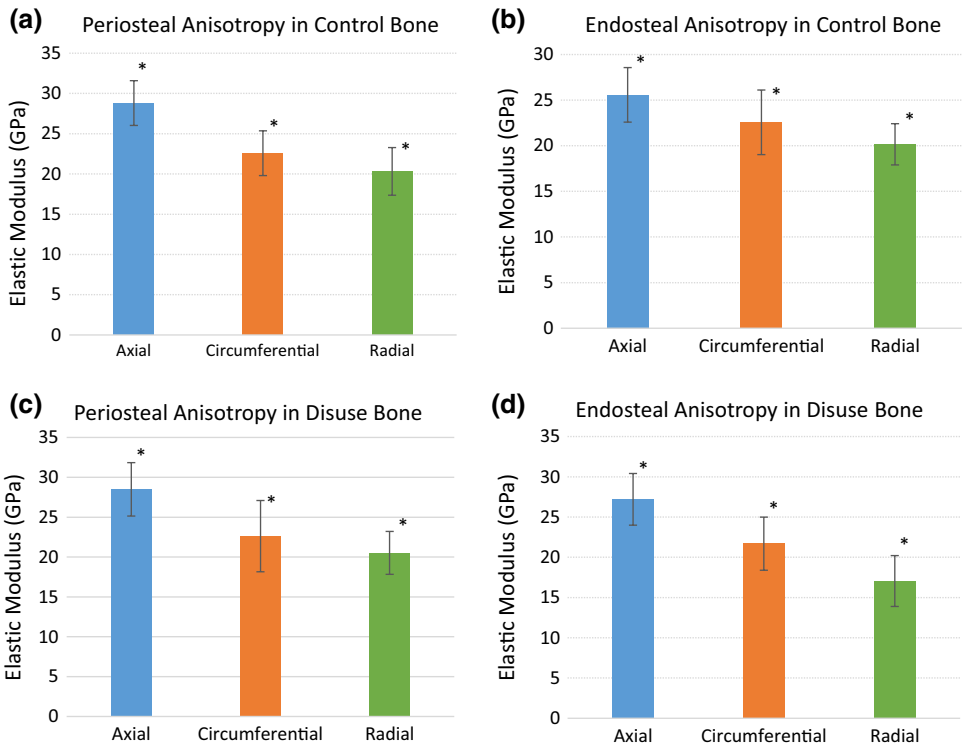

Fig. 3 **a** Graph charts displaying the periosteal elastic moduli values for both the control and disuse groups in the three orientations or the periosteal anisotropy. **b** Graph charts displaying the endosteal elastic moduli values in the control and disuse groups in all three orientations or the endosteal anisotropy. Statistical analysis performed in ANOVA (SPSS) and significance was set at 0.05. For both periosteum and endosteum regions, all orientations had statistically significant differences, confirmed with a Tukey pairwise post hoc analysis test

Variation of periosteal moduli in the orthogonal orientations between control and disuse groups

The elastic moduli of each orientation at the periosteal region were compared between the control and disuse groups as shown schematically in Fig. 4a. The results showed the statistically insignificant difference of the E values between the control and disuse group for all three orientations-radial ($p > 0.05$), circumferential ($p > 0.05$) and axial ($p > 0.05$).

Variation of endosteal moduli in the orthogonal orientations between control and disuse groups

The elastic moduli data of each orientation at the endosteal region was compared between the control and disuse groups as shown schematically in Fig. 4b. The results showed a statistically significant difference of E values in the radial ($p < 0.001$) and circumferential ($p < 0.001$) and the statistically insignificant difference in the axial orientation ($p > 0.05$).

Variation of periosteal Z/C, Z/R and C/R moduli ratios between control and disuse groups

The tests showed statistically insignificant differences for the periosteal Z/C and C/R ratios between the control and disuse groups ($p > 0.05$). But a statistically significant difference was concluded for the periosteal Z/R ratios between the control and disuse groups ($p < 0.05$), as shown in Fig. 5.

Variation of endosteal Z/C, Z/R and C/R moduli ratios between control and disuse groups

The tests showed statistically significant differences for the endosteal Z/C ($p < 0.001$), Z/R ($p < 0.001$) as well as C/R ($p < 0.05$) moduli ratios between the control and disuse groups as shown in Fig. 5.

Discussion

This study was undertaken to investigate the effects of bone remodeling from functional disuse of not just specific regions of the bone, but also in different orientations. Both periosteum as well as endosteum, at a lateral side of the cortical mid-tibia, were investigated with the use of nanoindentation, to evaluate changes in elastic moduli to give hints in elucidating the underlying bone remodeling process.

Bone anisotropy

The data from the control group (Fig. 3) showed that bones had highest elastic moduli in the axial orientation, which is in agreement with previous research by other groups who used nanoindentation for measuring the elastic modulus [50–52, 57]. Inside the bone, hydroxyapatite mineral deposition and orientation, as well as collagen fiber orientation, determine the mechanical modulus [58, 59]. Bone adapts itself to the mechanical loads it faces and remodels

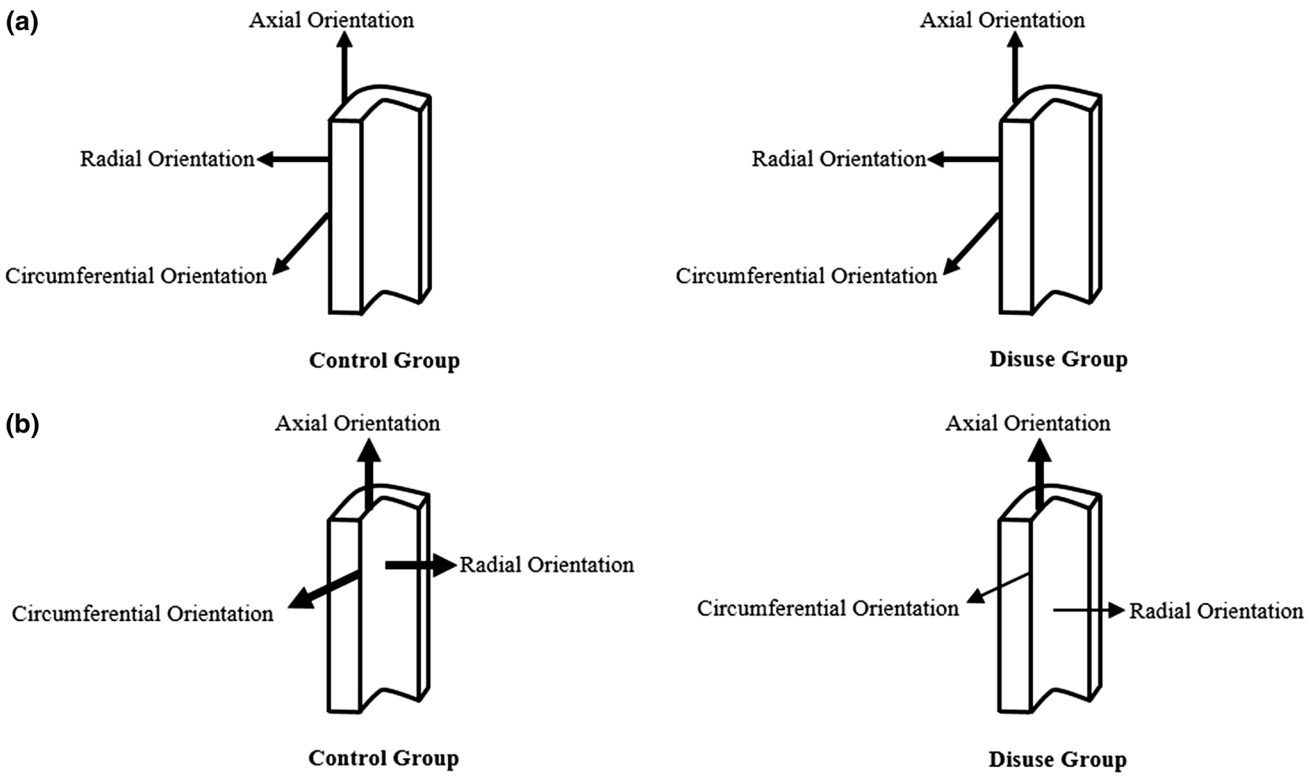

Fig. 4 **a** Schematic representing the damage from functional disuse for the periosteum. The image shows insignificant damage in all the three orientations from 1 month of hind limb suspension, by same sized arrows. **b** Schematic representing the damage from functional disuse for the endosteum. The image shows a significant reduction in the circumferential and radial orientations from 1 month of hind limb suspension. The comparison is made between control and disuse groups where a thin arrow represents an insignificant difference ($p > 0.05$), whereas a thick arrow represents a significant difference ($p < 0.05$)

accordingly [60, 61], also stated in Wolff's law and later modified by Frost [16, 62]. Strain-based remodeling theory suggests that bones remodel and form more bone to make it stronger in the orientation of higher strains [63]. Thereby with the theory, our results suggest that the load and strain distribution is maximum in the axial and least in the radial orientation at the cortical mid-tibia diaphysis. The trend is similar for both the periosteum and medullary endosteum layers, suggesting similar strain and load patterns experienced by both the regions. This result is in agreement with some of the results on the macro scale where a load anisotropy is presented [64, 65].

Variation of periosteal moduli and their ratios between control and disuse groups

Previous research on the macro scale has demonstrated that remodeling from functional disuse causes a loss of mechanical moduli due to alteration and reduction in mineral deposition, and an alteration in collagen fiber density and strength [66, 67]. In this study, separately investigating the periosteum region, shows that periosteal moduli in all orientations are unaffected from initial periods of functional disuse. No significant changes of principle orientations of elastic moduli at periosteum suggest that mineral and collagen fiber density was preserved. To account for the microarchitecture of the periosteum, ratio analysis of the moduli was also conducted for the periosteum. Significant differences between the groups were found for the Z/R ratio only. The Z/C and C/R ratios, however, remain unaffected from a month of disuse (Fig. 5). The analysis suggested the beginning of remodeling and only slight remodeling activity to have taken place along the periosteum.

Variation of endosteal moduli and their ratios between control and disuse groups

Reduction in micro-mechanical elastic moduli at the medullary endosteum hints towards possible resorption of the bone occurring along the endosteal region (Fig. 4b). This is in agreement with much of previous research, which has demonstrated that remodeling from functional disuse causes endosteal resorption [38]. The preservation of elastic moduli in the axial orientation, however, hinted at an insignificant loss in mineral and collagen fiber density. A diminution in mineral or collagen density would have resulted in an

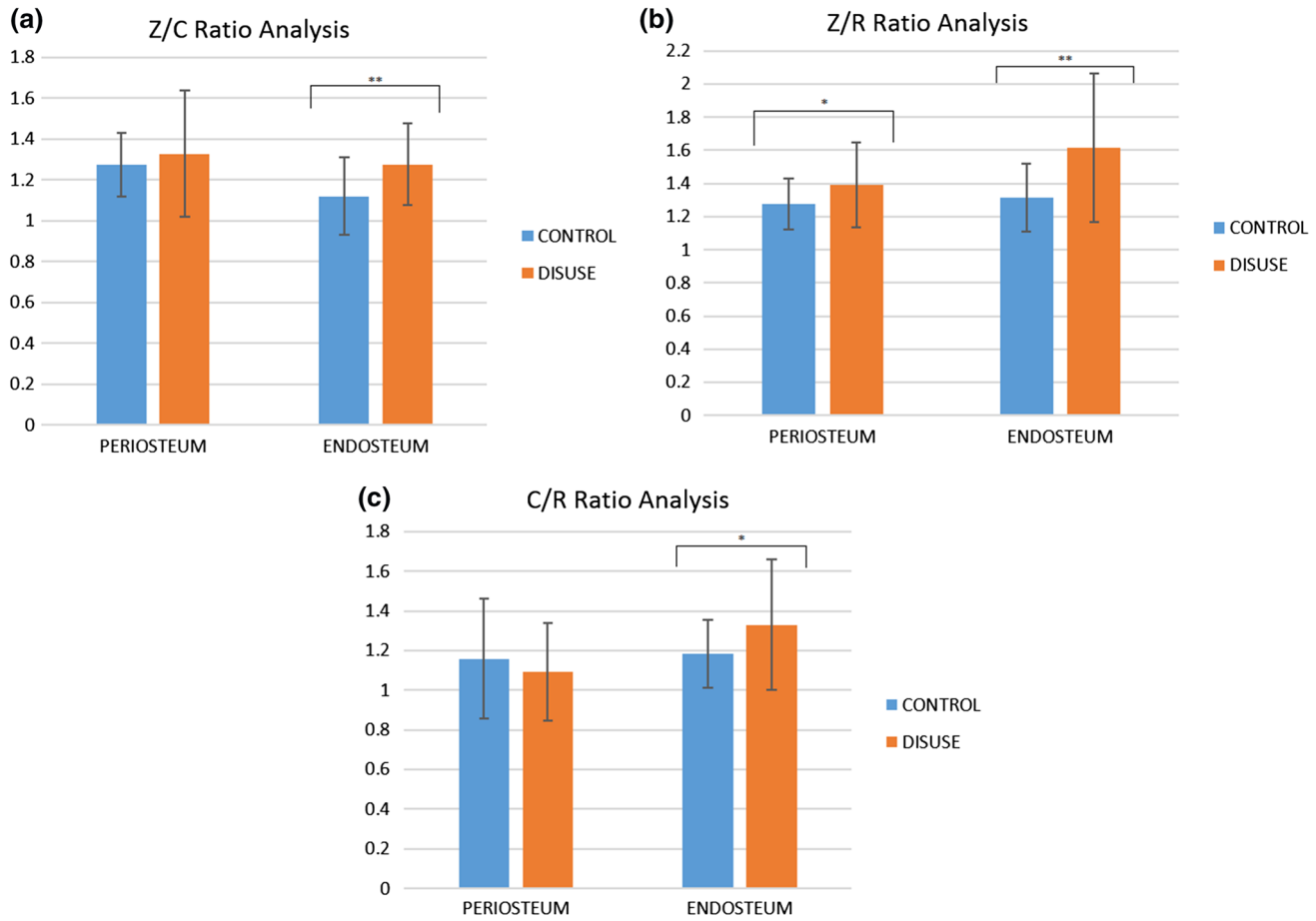

Fig. 5 Charts are showing the Z/C (**a**), Z/R (**b**) and C/R (**c**) ratio analysis for both periosteal and endosteal regions of bone between the control and disuse groups. *Represent $p < 0.05$, whereas **Represent $p < 0.001$

increased porosity of the bone, which would have resulted in a reduced modulus in all the three orientations. However, a significant change in all the three moduli ratios (Z/C, Z/R, C/R) between the control and disuse groups suggested significant microstructural remodeling of the endosteum. Thus, the results signify a remodeling in the orientations of the mineral lattice and collage fibers without an overall significant loss in density in the initial periods of functional disuse. Such impairment of bone microstructure could have resulted in a decrease in the mechanical moduli for the radial and circumferential orientations, leaving the elastic modulus along the axial orientation unaffected.

Site-specific bone micro-architecture alteration resulting from functional disuse

Collagen, the main organic component of the bone, is initially secreted in globular domains and finally stabilized by the formation of cross-links [68, 69], either enzymatic or non-enzymatic [70, 71]. Cross-linking is a major determinant of bone strength and fracture propagation [71–73] and is shown to have possible dependence on loading, age, and exercise for post-translational modifications [72, 74–77]. The orientation of collagen fibers and the cross-linking also govern the alignment of hydroxyapatite mineral crystals [70–72, 75].

Alterations in the organization of collagen fiber and packing of the mineral lattice may result in compromised bone moduli along specific orientations [71]. The results demonstrated region specific compromise of bone moduli, thus highlighting the importance of the day to day loading for the maintenance of the bone micro-architecture, collagen cross-linking and lattice structure. These results suggest the design of drugs against the deterioration of the bone micro-architecture. A loss in the quantity of bone mineral and collagen might be precluded if the structure is preserved. The study has a high clinical significance for studying the mechanotransduction pathways involved in the necessity of loading for the preservation of the geometric packaging of collagen and mineral lattice. The study also highlights the nature of the mechanotransduction

pathway keeping the periosteal region of the bone unaltered from initial periods of functional disuse.

Future direction

To further shed light on micro-bone remodeling from the effects of functional disuse on the bone micro-architecture, one of the immediate next steps would be to analyze the protein and mineral phases of the bone separately. Collagen fiber orientation can be assessed by studying the rotation of plane polarized light (PPL) at the periosteum and endosteum sites of nanoindentation for both control and disuse groups [71, 78]. Similarly, for investigating effects on bone mineral density distribution, backscatter electron imaging at the nanoindentation sites be adopted [66]. Another future work of the research will be to investigate the effects of functional disuse on other mechanical properties such as bone hardness.

Limitations

The study conducted had some limitations in the method and in the amount of data collected for forming the appropriate conclusion. For the methods, nanoindentation was carried out for measuring the mechanical properties after dehydration of the bone samples. Dehydrating the samples causes elastic moduli to increase and is a major limitation for any nanoindentation experiment [34, 79]. The other major limitation in forming a conclusion is that the study was conducted only for the lateral side of bone. As investigated earlier by the group, different sides in a bone cross-section remodel differently to disuse conditions [80]. To ascertain the initial structural remodeling of first the endosteum region, similar studies would also have to be conducted on the other sides (anterior, posterior and medial) of the bone as well.

Conclusion

While disuse adversely affects bone mechanical competence, the study showed that initial bone remodeling from osteopenia leads to an early alteration in the bone micro-architecture. The assessment of elastic moduli in the three orthogonal orientations and their ratios concluded that this effect on the bone micro-architecture, initially affected the medullary endosteal and not the periosteal layers of the bone.

Acknowledgements This work is kindly supported by the National Institute of Health (R01 AR52379 and R01AR61821), the US Army Medical Research and Materiel Command, The National Space Biomedical Research Institute through NASA contract NCC 9-58. I would also like to acknowledge Tony Zhang for his technical assistance.

Compliance with ethical standards

Conflict of interest The authors declare that there is no conflicts of interest to disclose in relation to this manuscript.

Ethical approval The experimental setting, data analyses, manuscript writing are all following ethical guidelines.

Informed consent There is no human nor live animal experiment involved in this study.

References

1. Burger EH, Klein-Nulend J (1999) Mechanotransduction in bone–role of the lacuno-canalicular network. FASEB J 13(Suppl):S101–S112
2. Qin YX, Lam H, Ferreri S, Rubin C (2010) Dynamic skeletal muscle stimulation and its potential in bone adaptation. J Musculoskelet Neuronal Interact 10:12–24
3. Qin YX, Rubin CT, McLeod KJ (1998) Nonlinear dependence of loading intensity and cycle number in the maintenance of bone mass and morphology. J Orthop Res 16:482–489. https://doi.org/10.1002/jor.1100160414
4. Weinbaum S, Cowin SC, Zeng Y (1994) A model for the excitation of osteocytes by mechanical loading-induced bone fluid shear stresses. J Biomech 27:339–360
5. Reich KM, Gay CV, Frangos JA (1990) Fluid shear stress as a mediator of osteoblast cyclic adenosine monophosphate production. J Cell Physiol 143:100–104. https://doi.org/10.1002/jcp.1041430113
6. Knothe Tate ML, Niederer P, Knothe U (1998) In vivo tracer transport through the lacunocanalicular system of rat bone in an environment devoid of mechanical loading. Bone 22:107–117. https://doi.org/10.1016/S8756-3282(97)00234-2
7. Rubin J, Biskobing D, Fan X, Rubin C, McLeod K, Taylor WR (1997) Pressure regulates osteoclast formation and MCSF expression in marrow culture. J Cell Physiol 170:81–87. https://doi.org/10.1002/(SICI)1097-4652(199701)170:1%3c81:AID-JCP9%3e3.0.CO;2-H
8. Huang C, Ogawa R (2010) Mechanotransduction in bone repair and regeneration. FASEB J 24:3625–3632. https://doi.org/10.1096/fj.10-157370fj.10-157370
9. Turner CH, Forwood MR, Otter MW (1994) Mechanotransduction in bone: do bone cells act as sensors of fluid flow? FASEB J 8:875–878
10. Donaldson CL, Hulley SB, Vogel JM, Hattner RS, Bayers JH, McMillan DE (1970) Effect of prolonged bed rest on bone mineral. Metabolism 19:1071–1084
11. Huang C, Holfeld J, Schaden W, Orgill D, Ogawa R (2013) Mechanotherapy: revisiting physical therapy and recruiting mechanobiology for a new era in medicine. Trends Mol Med 19:555–564. https://doi.org/10.1016/j.molmed.2013.05.005S1471-4914(13)00092-0
12. Manske SL, Lorincz CR, Zernicke RF (2009) Bone health: part 2, physical activity. Sports Health 1:341–346. https://doi.org/10.1177/1941738109338823 10.1177_1941738109338823
13. Rubin CT, Lanyon LE (1987) Kappa delta award paper. osteoregulatory nature of mechanical stimuli: function as a determinant for adaptive remodeling in bone. J Orthop Res 5:300–310. https://doi.org/10.1002/jor.1100050217
14. van der Meulen MC, Morgan TG, Yang X, Baldini TH, Myers ER, Wright TM, Bostrom MP (2006) Cancellous bone adaptation to

in vivo loading in a rabbit model. Bone 38:871–877. https://doi.org/10.1016/j.bone.2005.11.026
15. Wallace JM, Ron MS, Kohn DH (2009) Short-term exercise in mice increases tibial post-yield mechanical properties while 2 weeks of latency following exercise increases tissue-level strength. Calcif Tissue Int 84:297–304. https://doi.org/10.1007/s00223-009-9228-8
16. Wolf JH (1995) Julis Wolff and his "law of bone remodeling" (in ger). Orthopade (Julius Wolff und sein "Gesetz der Transformation der Knochen") 24:378–386
17. Gross TS, Rubin CT (1995) Uniformity of resorptive bone loss induced by disuse. J Orthop Res 13:708–714. https://doi.org/10.1002/jor.1100130510
18. Kaneps AJ, Stover SM, Lane NE (1997) Changes in canine cortical and cancellous bone mechanical properties following immobilization and remobilization with exercise. Bone 21:419–423. https://doi.org/10.1016/S8756-3282(97)00167-1
19. Li CY, Price C, Delisser K, Nasser P, Laudier D, Clement M, Jepsen KJ, Schaffler MB (2005) Long-term disuse osteoporosis seems less sensitive to bisphosphonate treatment than other osteoporosis. J Bone Miner Res 20:117–124. https://doi.org/10.1359/JBMR.041010
20. Lau RY, Guo X (2011) A review on current osteoporosis research: with special focus on disuse bone loss. J Osteoporos 2011:293808. https://doi.org/10.4061/2011/293808
21. Weiner S, Traub W, Wagner HD (1999) Lamellar bone: structure-function relations. J Struct Biol 126:241–255. https://doi.org/10.1006/jsbi.1999.4107
22. Manjubala I, Liu Y, Epari DR, Roschger P, Schell H, Fratzl P, Duda GN (2009) Spatial and temporal variations of mechanical properties and mineral content of the external callus during bone healing. Bone 45:185–192. https://doi.org/10.1016/j.bone.2009.04.249S8756-3282(09)01565-8
23. Martin RB, Boardman DL (1993) The effects of collagen fiber orientation, porosity, density, and mineralization on bovine cortical bone bending properties. J Biomech 26:1047–1054
24. Martin RB, Ishida J (1989) The relative effects of collagen fiber orientation, porosity, density, and mineralization on bone strength. J Biomech 22:419–426
25. Skedros JG, Dayton MR, Sybrowsky CL, Bloebaum RD, Bachus KN (2006) The influence of collagen fiber orientation and other histocompositional characteristics on the mechanical properties of equine cortical bone. J Exp Biol 209:3025–3042. https://doi.org/10.1242/jeb.02304
26. Roberts BJ, Thrall E, Muller JA, Bouxsein ML (2010) Comparison of hip fracture risk prediction by femoral aBMD to experimentally measured factor of risk. Bone 46:742–746. https://doi.org/10.1016/j.bone.2009.10.020S8756-3282(09)01988-7
27. Bouxsein ML, Seeman E (2009) Quantifying the material and structural determinants of bone strength. Best Pract Res Clin Rheumatol 23:741–753. https://doi.org/10.1016/j.berh.2009.09.008S1521-6942(09)00101-6
28. Gao J, Gong H, Huang X, Fang J, Zhu D, Fan Y (2013) Relationship between microstructure, material distribution, and mechanical properties of sheep tibia during fracture healing process. Int J Med Sci 10:1560–1569. https://doi.org/10.7150/ijms.6611ijmsv10p1560
29. Yeni YN, Wu B, Huang L, Oravec D (2013) Mechanical loading causes detectable changes in morphometric measures of trabecular structure in human cancellous bone. J Biomech Eng 135:54505. https://doi.org/10.1115/1.40241361681767
30. Currey JD (2003) The many adaptations of bone. J Biomech 36:1487–1495. https://doi.org/10.1016/S0021-9290(03)00124-6
31. Rho JY, Kuhn-Spearing L, Zioupos P (1998) Mechanical properties and the hierarchical structure of bone. Med Eng Phys 20:92–102. https://doi.org/10.1016/S1350-4533(98)000071
32. Courtland HW, Nasser P, Goldstone AB, Spevak L, Boskey AL, Jepsen KJ (2008) Fourier transform infrared imaging microspectroscopy and tissue-level mechanical testing reveal intraspecies variation in mouse bone mineral and matrix composition. Calcif Tissue Int 83:342–353. https://doi.org/10.1007/s00223-008-9176-8
33. Donnelly E, Boskey AL, Baker SP, van der Meulen MC (2010) Effects of tissue age on bone tissue material composition and nanomechanical properties in the rat cortex. J Biomed Mater Res A 92:1048–1056. https://doi.org/10.1002/jbm.a.32442
34. Lewis G, Nyman JS (2008) The use of nanoindentation for characterizing the properties of mineralized hard tissues: state-of-the art review. J Biomed Mater Res B Appl Biomater 87:286–301. https://doi.org/10.1002/jbm.b.31092
35. Clarke B (2008) Normal bone anatomy and physiology. Clin J Am Soc Nephrol 3(Suppl 3):S131–S139. https://doi.org/10.2215/CJN.041512063/Supplement_3/S131
36. Ved N, Haller JO (2002) Periosteal reaction with normal-appearing underlying bone: a child abuse mimicker. Emerg Radiol 9:278–282. https://doi.org/10.1007/s10140-002-0252-5
37. Dwek JR (2010) The periosteum: what is it, where is it, and what mimics it in its absence? Skeletal Radiol 39:319–323. https://doi.org/10.1007/s00256-009-0849-9
38. Seeman E (2003) Reduced bone formation and increased bone resorption: rational targets for the treatment of osteoporosis. Osteoporos Int 14(Suppl 3):S2–S8. https://doi.org/10.1007/s00198-002-1340-9
39. Szulc P, Seeman E, Duboeuf F, Sornay-Rendu E, Delmas PD (2006) Bone fragility: failure of periosteal apposition to compensate for increased endocortical resorption in postmenopausal women. J Bone Miner Res 21:1856–1863. https://doi.org/10.1359/jbmr.060904
40. LaMothe JM, Hamilton NH, Zernicke RF (2005) Strain rate influences periosteal adaptation in mature bone. Med Eng Phys 27:277–284. https://doi.org/10.1016/j.medengphy.2004.04.012
41. Kodama Y, Umemura Y, Nagasawa S, Beamer WG, Donahue LR, Rosen CR, Baylink DJ, Farley JR (2000) Exercise and mechanical loading increase periosteal bone formation and whole bone strength in C57BL/6 J mice but not in C3H/Hej mice. Calcif Tissue Int 66:298–306. https://doi.org/10.1007/s002230010060
42. Hoffmeister BK, Smith SR, Handley SM, Rho JY (2000) Anisotropy of Young's modulus of human tibial cortical bone. Med Biol Eng Comput 38:333–338
43. Angker L, Swain MV, Kilpatrick N (2005) Characterising the micro-mechanical behaviour of the carious dentine of primary teeth using nano-indentation. J Biomech 38:1535–1542. https://doi.org/10.1016/j.jbiomech.2004.07.012
44. Ebenstein DM, Pruitt LA (2004) Nanoindentation of soft hydrated materials for application to vascular tissues. J Biomed Mater Res A 69:222–232. https://doi.org/10.1002/jbm.a.20096
45. Fan Z, Swadener JG, Rho JY, Roy ME, Pharr GM (2002) Anisotropic properties of human tibial cortical bone as measured by nanoindentation. J Orthop Res 20:806–810. https://doi.org/10.1016/S0736-0266(01)00186-3
46. Hoffler CE, Guo XE, Zysset PK, Goldstein SA (2005) An application of nanoindentation technique to measure bone tissue Lamellae properties. J Biomech Eng 127:1046–1053
47. Imbert L, Auregan JC, Pernelle K, Hoc T (2014) Mechanical and mineral properties of osteogenesis imperfecta human bones at the tissue level. Bone 65:18–24. https://doi.org/10.1016/j.bone.2014.04.030S8756-3282(14)00165-3
48. Pathak S, Vachhani SJ, Jepsen KJ, Goldman HM, Kalidindi SR (2012) Assessment of lamellar level properties in mouse bone utilizing a novel spherical nanoindentation data analysis method. J Mech Behav Biomed Mater 13:102–117. https://doi.org/10.1016/j.jmbbm.2012.03.018S1751-6161(12)00107-5

49. Khandaker M, Ekwaro-Osire S (2013) Weibull analysis of fracture test data on bovine cortical bone: influence of orientation. Int J Biomater 2013:639841. https://doi.org/10.1155/2013/639841
50. Carnelli D, Vena P, Dao M, Ortiz C, Contro R (2013) Orientation and size-dependent mechanical modulation within individual secondary osteons in cortical bone tissue. J R Soc Interface 10:20120953. https://doi.org/10.1098/rsif.2012.0953rsif.2012.0953
51. Faingold A, Cohen SR, Wagner HD (2012) Nanoindentation of osteonal bone lamellae. J Mech Behav Biomed Mater 9:198–206. https://doi.org/10.1016/j.jmbbm.2012.01.014S1751-6161(12)00034-3
52. Franzoso G, Zysset PK (2009) Elastic anisotropy of human cortical bone secondary osteons measured by nanoindentation. J Biomech Eng 131:021001. https://doi.org/10.1115/1.3005162
53. Reisinger AG, Pahr DH, Zysset PK (2011) Principal stiffness orientation and degree of anisotropy of human osteons based on nanoindentation in three distinct planes. J Mech Behav Biomed Mater 4:2113–2127. https://doi.org/10.1016/j.jmbbm.2011.07.010S1751-6161(11)00197-4
54. Hu M, Cheng J, Qin YX (2012) Dynamic hydraulic flow stimulation on mitigation of trabecular bone loss in a rat functional disuse model. Bone 51:819–825. https://doi.org/10.1016/j.bone.2012.06.030S8756-3282(12)00963-5
55. Milstead JR, Simske SJ, Bateman TA (2004) Spaceflight and hindlimb suspension disuse models in mice (in eng). Biomed Sci Instrum 40:105–110
56. Hoc T, Henry L, Verdier M, Aubry D, Sedel L, Meunier A (2006) Effect of microstructure on the mechanical properties of Haversian cortical bone. Bone 36:466–474
57. Faingold A, Cohen SR, Shahar R, Weiner S, Rapoport L, Wagner HD (2014) The effect of hydration on mechanical anisotropy, topography and fibril organization of the osteonal lamellae. J Biomech 47:367–372. https://doi.org/10.1016/j.jbiomech.2013.11.022S0021-9290(13)00574-5
58. Knott L, Bailey AJ (1998) Collagen cross-links in mineralizing tissues: a review of their chemistry, function, and clinical relevance. Bone 22:181–187. https://doi.org/10.1016/S8756-3282(97)00279-2
59. Viguet-Carrin S, Garnero P, Delmas PD (2006) The role of collagen in bone strength. Osteoporos Int 17:319–336. https://doi.org/10.1007/s00198-005-2035-9
60. Marzban A, Canavan P, Warner G, Vaziri A, Nayeb-Hashemi H (2012) Parametric investigation of load-induced structure remodeling in the proximal femur. Proc Inst Mech Eng H 226:450–460. https://doi.org/10.1177/0954411912444067
61. Meakin LB, Price JS, Lanyon LE (2014) The contribution of experimental in vivo models to understanding the mechanisms of adaptation to mechanical loading in bone. Front Endocrinol (Lausanne) 5:154. https://doi.org/10.3389/fendo.2014.00154
62. Frost HM (1994) Wolff's Law and bone's structural adaptations to mechanical usage: an overview for clinicians. Angle Orthod 64:175–188. https://doi.org/10.1043/0003-3219(1994)064%3c0175:WLABSA%3e2.0.CO;2
63. Main RP (2007) Ontogenetic relationships between in vivo strain environment, bone histomorphometry and growth in the goat radius. J Anat 210:272–293. https://doi.org/10.1111/j.1469-7580.2007.00696.x
64. Cristofolini L, Angeli E, Juszczyk JM, Juszczyk MM (2013) Shape and function of the diaphysis of the human tibia. J Biomech 46:1882–1892. https://doi.org/10.1016/j.jbiomech.2013.04.026S0021-9290(13)00220-0
65. Funk JR, Crandall JR (2006) Calculation of tibial loading using strain gauges. Biomed Sci Instrum 42:160–165
66. Boskey AL (2006) Assessment of bone mineral and matrix using backscatter electron imaging and FTIR imaging. Curr Osteoporos Rep 4:71–75
67. Tranquilli Leali P, Doria C, Zachos A, Ruggiu A, Milia F, Barca F (2009) Bone fragility: current reviews and clinical features. Clin Cases Miner Bone Metab 6:109–113
68. Saito M, Marumo K (2010) Collagen cross-links as a determinant of bone quality: a possible explanation for bone fragility in aging, osteoporosis, and diabetes mellitus. Osteoporos Int 21:195–214. https://doi.org/10.1007/s00198-009-1066-z
69. Saito M, Marumo K (2010) Musculoskeletal rehabilitation and bone. Mechanical stress and bone quality: do mechanical stimuli alter collagen cross-link formation in bone? "Yes" (in jpn). Clin Calcium 20:520–528 **(pii: CliCa1004520528 1004520528)**
70. Sroga GE, Vashishth D (2012) Effects of bone matrix proteins on fracture and fragility in osteoporosis. Curr Osteoporos Rep 10:141–150. https://doi.org/10.1007/s11914-012-0103-6
71. Vashishth D, Gibson GJ, Khoury JI, Schaffler MB, Kimura J, Fyhrie DP (2001) Influence of nonenzymatic glycation on biomechanical properties of cortical bone. Bone 28:195–201. https://doi.org/10.1016/S8756-3282(00)00434-8
72. Boskey AL, Coleman R (2010) Aging and bone. J Dent Res 89:1333–1348. https://doi.org/10.1177/0022034510377791
73. Tang SY, Vashishth D (2011) The relative contributions of non-enzymatic glycation and cortical porosity on the fracture toughness of aging bone. J Biomech 44:330–336. https://doi.org/10.1016/j.jbiomech.2010.10.016S0021-9290(10)00568-3
74. Brama PA, Bank RA, Tekoppele JM, Van Weeren PR (2001) Training affects the collagen framework of subchondral bone in foals. Vet J 162:24–32. https://doi.org/10.1053/tvjl.2001.0570S1090023301905702
75. Paschalis EP, Shane E, Lyritis G, Skarantavos G, Mendelsohn R, Boskey AL (2004) Bone fragility and collagen cross-links. J Bone Miner Res 19:2000–2004. https://doi.org/10.1359/JBMR.040820
76. Salem GJ, Zernicke RF, Martinez DA, Vailas AC (1993) Adaptations of immature trabecular bone to moderate exercise: geometrical, biochemical, and biomechanical correlates. Bone 14:647–654
77. van de Lest CH, Brama PA, van Weeren PR (2003) The influence of exercise on bone morphogenic enzyme activity of immature equine subchondral bone. Biorheology 40:377–382
78. Bromage TG, Goldman HM, McFarlin SC, Warshaw J, Boyde A, Riggs CM (2003) Circularly polarized light standards for investigations of collagen fiber orientation in bone. Anat Rec B New Anat 274:157–168. https://doi.org/10.1002/ar.b.10031
79. Nyman JS, Roy A, Shen X, Acuna RL, Tyler JH, Wang X (2006) The influence of water removal on the strength and toughness of cortical bone. J Biomech 39:931–938. https://doi.org/10.1016/j.jbiomech.2005.01.012
80. Grover K, Lin L, Hu M, Muir J, Qin YX (2016) Spatial distribution and remodeling of elastic modulus of bone in microregime as prediction of early stage osteoporosis. J Biomech 49:161–166. https://doi.org/10.1016/j.jbiomech.2015.11.052S0021-9290(15)00694-6